

Layered manganates from soft-templates: preparation, characterization and enhanced dye demethylation capabilities

Pedro Tartaj*

Received 24th April 2012, Accepted 4th July 2012

DOI: 10.1039/c2jm32583g

A soft-template method for the synthesis of layered manganate (K_xMnO_2 , birnessites) compounds with a relatively good control at the nanoscale regime on the number of octahedral layers (thickness) is described. The soft-template method is based on the stabilization of reverse micelles at moderate temperatures and the optimization of parameters to modulate the size of the templates while still preserving their stability during the formation of layered manganates. Degradation experiments of a model system (methylene blue) using the birnessites here reported have shown efficient demethylation in the absence of oxidants for aqueous suspensions made of non-dried birnessites containing the fewest number of layers. The observed strong thickness and aggregation dependence (*i.e.* dependence on exposed surfaces) for demethylation explains why particulate birnessites have only been considered for dye sequestration and not as an efficient demethylation agent in the absence of oxidants. Finally, when compared to electrodeposited thin films, the higher loading capabilities of the colloidal suspensions here prepared have made it possible to demethylate larger amounts of methylene blue at a similar time.

1. Introduction

The redox properties of layered transition-metal oxides have been routinely used for environmental and energy applications.^{1–3} These oxides, however, when operating at highly or even moderately active material loads (say for example when processed in particulate form) have low capabilities associated with diffusion/contact problems. Indeed, layered transition-metal oxides when processed as thin films can approach theoretical capabilities especially when redox processes are involved,^{4,5} but thin films' applicability is limited by low active material loadings. Hereafter we report a soft-template method based on the Igepal/organic solvent/water system for the controlled synthesis of layered manganates (K_xMnO_2 , birnessite). The method allows a good control at the nanoscale regime on the number of octahedral layers (thickness) without altering chemical and basal spacing. We show, for a model system (methylene blue), that aqueous suspensions containing the birnessites here prepared can demethylate larger amounts of this colorant compared to the homologous electrodeposited thin films.

Among organic pollutants, organic dyes used in a broad variety of applications represent a real environmental problem and particularly methylene blue (MB) is the most important basic cationic dye. There is consensus in the literature that *N*-demethylation of auxochromic alkylamine groups is involved in the first stages of MB degradation.^{6,7} Discoloration and blue

shifts make *N*-demethylation easily to follow by UV/Vis spectrophotometry. Therefore, from a practical point of view, the use of MB assures relatively rapid checking for demethylation and reliable comparisons between materials (*i.e.* demethylation of MB can be considered a model system). MB in the presence of manganese oxides/hydroxides is usually degraded in combination with oxidants (H_2O_2 , *tert*-butyl hydroperoxide, *etc.*).^{6–9} Recent studies on electrodeposited layered manganate birnessite (K_xMnO_2) thin films, however, have shown that MB demethylation can take place even in the absence of oxidants at relatively short times (3 h).⁷ Showing the same effect in colloidal birnessites could open the possibility of moderately and highly active material loadings for demethylation of MB. Therefore, we understand that implementing a method to synthesize particulate birnessites with a relatively good control at the nanoscale regime on the number of octahedral layers (thickness) together with a simple, fast, yet robust method of checking degradation capabilities (methylene blue demethylation) has practical and fundamental interest. Demethylation of a cationic dye is of practical interest while the relatively good control at the nanoscale regime in a layered compound can shed some light on the different factors that cause the lower performance of particulate materials when compared to thin films.

There are many scientific reports that describe synthetic routes to produce K-birnessites.^{1,10–14} Precipitation routes usually involve not only the oxidation of aqueous Mn^{2+} cations but also the oxidation of amorphous solid precursors *via* the redox reaction between Mn^{2+} and MnO_4^- .^{1,16–18} Sol–gel synthesis usually involves various sugars and other organic polyalcohols as well as further heating to develop good crystallinity and remove

Instituto de Ciencia de Materiales de Madrid (CSIC), Campus Universitario de Cantoblanco 28049, Madrid, Spain. E-mail: ptartaj@icmm.csic.es

the organic additives.¹⁵ Recently, K-birnessites were prepared by dispersing monosheets in solutions containing K⁺ cations.^{13,19} To our knowledge none of these methods are able to produce a satisfactory control on the number of manganate octahedral layers together with a simultaneous control on chemical composition and basal spacing for colloidal K-birnessites. Here it is worth noting that we are not interested in methods that involve the preparation of birnessite in the presence of large cations. MB is a cationic dye, and there are numerous pieces of evidence that surface mechanisms are involved in the oxidative degradation of organic compounds by manganese oxides.¹⁶ Large cations can compete with MB for the adsorption sites lowering demethylation efficiencies (as better described in the Results and discussion section, lower efficiencies were detected by using a cationic polyelectrolyte).

As mentioned above a soft-template method based on the Igepal/organic solvent/water system has been selected in this work for the controlled synthesis of colloidal K-birnessites. Microemulsions in the system Igepal/cyclohexane/water have been routinely used to produce isotropic structures.¹⁷ Less frequently, however, is to exploit the fact that Igepal can form lamellar-like structures especially in some solvents such as heptane and decane.¹⁸ Furthermore, destabilization (say for example by the addition of an excess of water or by lowering the temperature) can go through the formation of interconnected lamellar-like structures.¹⁹ Soft lamellar structures are flexible and can easily accommodate the growth of isotropic structures.^{19,20} However, we are of the opinion that they will adapt better if the material itself has a tendency to grow in a lamellar structure as is the case of K-birnessites.

2. Experimental section

2.1. Chemicals

All chemical reactants (purity, >99%) were purchased from Sigma Aldrich. Mn(NO₃)₂·4H₂O, H₂O₂ (50%), NH₄S₂O₇, and KOH were used as precursors. Igepal CO-520 was used as a surfactant. Cyclohexane/heptane/decane dehydrated with zeolites were used as the continuous oil phase. Methylene blue, KH₂PO₄ and NaH₂PO₄ were used for demethylation studies.

2.2. Soft-template optimization

The optimization of conditions to obtain adequate soft-templates was carried out by temperature-dependent dynamic light scattering experiments (Nanosizer ZS, Malvern Instruments). Mixing of the components was carried out at room temperature under magnetic stirring in closed beakers. Then the mixtures were brought to 60 °C to assure the dissolution of the inorganic components. An aliquot was transferred for temperature-dependent dynamic light scattering experiments (the temperature of the cell compartment was 60 °C). Changes in hydrodynamic sizes with temperature were thus registered on cooling. For some conditions the destabilization of microemulsions was observed at 60 °C. If so, the same protocol was applied lowering the maximum temperature in 5 °C steps. Adequate conditions were found if the organic solvent contained cyclohexane–heptane mixtures (50 vol%, checked in a range that changes in a 25% step) and among four different Igepal

surfactants (CO-210; CO-520; CA-520; and CO-720), Igepal CO-520 at a 0.2 M concentration was used. Heptane and decane are known to favor lamellar-like structures; however, Mn salt solubility *via* reverse micelle formation in these pure solvents or in cyclohexane–decane mixtures was very low, and therefore a mixture of cyclohexane–heptane was used. The aqueous volume was set to 3% as the temperature range for microemulsion formation (single phases) and solubility of Mn salts were maximized. For a 3 vol% of aqueous component, this temperature range extends from 60 to 35 °C for the highest amount of Mn salts that can be dissolved (~0.07 M which is equivalent to 2.3 M in the aqueous component). For higher aqueous contents the temperature range for stability of microemulsions is reduced because high temperature destabilization takes place. At lower aqueous contents the solubility of Mn salts is low.

2.3. Soft-template assisted synthesis of birnessites

We find it mandatory to remark that for security and technical issues (bubbling of H₂O₂), we have carried out all the experiments in 250 or 500 mL closed beakers (50/100 mL of solution, respectively) and H₂O₂ concentration was restricted to 0.12 M for a KOH concentration of 0.47 M (concentrations referred to the total content). Hydrogen peroxide in acid medium can even reduce permanganate (MnO₄⁻) to Mn²⁺ cations (i.e. the acidity provided by the H₂O₂ itself makes solutions containing Mn²⁺ salts stable). However, H₂O₂ in basic medium (i.e. after addition of KOH) decomposes into water and gaseous oxygen (bubbling).

In a typical experiment 50/100 mL (100 mL for the lowest Mn concentrations) of a mixture containing the organic solvent (cyclohexane–heptane, 50 vol%), Igepal Co-520 (0.2 M), the aqueous component (3 vol%) and the reactants were prepared at room temperature under strong magnetic stirring in closed beakers. Then to assure equilibrium at 45 °C, the Mn salt was dissolved at 55 °C/15 min and the temperature was lowered to 45 °C in 30 min. In order to avoid Mn₃O₄ formation in the samples with the higher Mn concentrations (0.05 and 0.065 M), NH₄S₂O₇ was added once the microemulsion reached 45 °C. NH₄S₂O₇ dissolves during the 30 min that the microemulsion remains at this temperature before KOH addition. After 30 min at 45 °C, the appropriate volume of a KOH 14 M solution was rapidly added (*note that the container was kept open during addition of the KOH solution for security reasons associated with bubbling*). After 24 h the suspension was centrifuged at 1000 g for 10 minutes to discard the sediment. The supernatant was destabilized with isopropanol, centrifuged and washed (stirring 30 min) several times (twice with EtOH/water and 3 times with water) and redispersed in water for storage. An aliquot of these suspensions was centrifuged and dried for chemical analyses or for some methylene blue degradation studies involving dried samples.

2.4. Sample characterization

Temperature-dependent dynamic light scattering (DLS) experiments were carried out in a Nanosizer ZS (Malvern Instruments). X-Ray diffraction (XRD) patterns were collected from 5 to 50° (2θ) by using a Bruker D8 Advance instrument with CuKα radiation (λ = 0.15406 nm) and a SOLX detector

(postdiscriminator of fluorescence) operating at 40 kV and 30 mA. The crystal domain size was determined from the X-ray profiles following the Scherrer equation by using the DIFRAC-PLUS EVA software (BRUKER AXS). For estimation of the full width at half maximum the patterns were registered 5 different times. Basal spacing was determined using the same software and Si powder was used as an internal standard to correct the position of the peaks. For crystal size and basal spacing determination, the XRD patterns were registered with 20 s of accumulation time in the regions where the birnessite (001) peaks appear. The morphology of the obtained samples was studied with a JEOL transmission electron microscope working at 200 keV. Selective area diffraction patterns were taken using the same instrument. The chemical composition of samples was determined by ICP (Perkin Elmer Optima 2100 DV) and thermal analysis (Seiko EXSTAR 6300). For MB degradation studies the UV/Vis spectra were registered in a Perkin Elmer Lambda 35.

3. Results and discussion

3.1. Preparation and characterization of samples

Fig. 1 shows the evolution of micelle size as a function of Mn concentration and temperature for optimal conditions (see Experimental section for technical details). For K-birnessite synthesis, setting a constant temperature for the reaction increases the probability to produce these materials with similar chemical and basal spacing (the range of thermodynamic stability of hydrated forms such as birnessites is strongly dependent on temperature). Besides, we are dealing with very sensitive systems. Taking into consideration these two factors we set the working temperature at 45 °C. At this temperature significant differences in the micelle size are observed (thicknesses are thus prone to change) while still working in the middle of the stability window (Fig. 1, Table 1). At 45 °C, the size of reverse micelles increases with the increase in Mn concentration except for the lower Mn concentrations where such variations are not significant (Fig. 1, Table 1). In fact, similar values were obtained

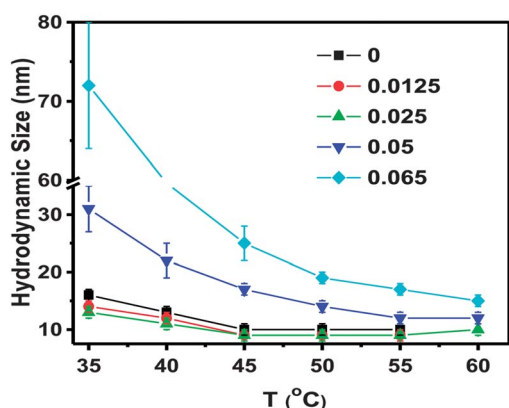


Fig. 1 Evolution of hydrodynamic size as a function of Mn concentration and temperature (cyclohexane–heptane, 50 vol%; Igepal CO-520, 0.2 M; aqueous volume = 3%; $\text{NH}_4\text{S}_2\text{O}_7 = 0.02 \text{ M}$). The curve was registered on cooling to assure equilibrium conditions. Note the split in the y axis to better display size differences at the working temperature (45 °C).

for micelles prepared in the absence of Mn (Fig. 1, Table 1). This result suggests that for Mn concentrations below about 0.025 M the micelle size reflects the contribution of both the aqueous content itself and the contribution of the dissolved $\text{NH}_4\text{S}_2\text{O}_7$ salt.

Based on the characteristics of the soft-templates at 45 °C (Fig. 1 and Table 1) our initial assumptions to try to attain a relatively good control at the nanoscale regime on the number of manganate octahedral layers (thickness) were: (a) thickness primarily increases with micelle size except for the lowest Mn concentrations (templating effect) – strictly speaking with the aqueous micellar cavity size, which we define as the hydrodynamic size minus twice the surfactant thickness (1–1.5 nm is about the thickness of the surfactant layer)²¹ and (b) large aqueous micellar cavities can produce thicker birnessites but also thinner ones. This hypothesis suggests that the reactant concentrations also modulate the birnessite thickness. Based on nucleation theory, we assumed that higher oxidation rates (high oxidant/Mn ratios) could lead to a reduction in thickness associated with faster reactions. Addition of KOH (see Experimental section for technical details) under these guidelines made it possible to modulate the birnessite thickness from 3.0 to 8.1 nm (Table 1, Fig. 2A) without altering the chemical composition ($\text{K}_{0.3}\text{MnO}_2 \cdot 0.6\text{H}_2\text{O}$) and basal spacing (0.72–0.73 nm).

The colloidal nature (particle sizes with an average of around 150 nm) of the non-dried birnessites was assessed by dynamic light scattering (Fig. 2B). BET (Brunauer–Emmett–Teller) surface area determination and scanning electron microscopy characterization were discarded as drying of the material may alter the surface area and microstructure (referred to as the assembly of primary units in different morphologies). In fact, as we better describe below demethylation did not take place if experiments were made in dried samples, which clearly indicates aggregation after drying (*i.e.* less active surface area exposed). In any case, the transmission electron microscopy (TEM) in dried samples clearly shows us the presence of a layered compound in the form of a birnessite aggregate. TEM shows an aggregate with the typical corrugation associated with ultrathin sheet-like materials, that is, with a layered compound (Fig. 2C). The disordered arrangement of the aggregate formed by thin nano-sheets (polycrystal-like assembly) gives a ring-type diffraction pattern, which can be indexed within the birnessite structure (Fig. 2D).

3.2. Analysis of experimental errors

An analysis of errors is mandatory as we are dealing with relatively sensitive synthesis routes. Fig. 1 for example indicates that at 45 °C errors can be larger for high Mn concentrations ($\Delta\text{size}/\Delta T$ increases). Errors, however, are minimized by the layered structure of the material itself especially as thickness decreases. We cannot produce birnessites with a non-integer number of layers (*i.e.* layered structures introduce quantization). As the thickness decreases, we come close to the minimum number of layers that a birnessite can contain, and polydispersity (referred to the possible presence of birnessites with different number of layers) is low. Errors were not detected at small thicknesses, and the maximum error was limited to around a bilayer (Table 1). As we will better describe later, the better demethylation capabilities are found in the samples with the smallest thicknesses (no errors,

Table 1 Reactant concentrations (mol L⁻¹ referred to the total volume) used to prepare birnessites between 5 and 12 layers. Micelle and aqueous micellar cavity hydrodynamic sizes at 45 °C. As mentioned in the main text the micellar cavity is the hydrodynamic size minus twice the surfactant thickness (2–3 nm). Crystal sizes, basal spacing and number of octahedral layers (1 + (crystal size/basal spacing)). Errors in the number of layers were derived from five or ten experiments (if errors were detected during the first 5 experiments we carried out 5 additional experiments)

[Mn]	[H ₂ O ₂]	[KOH]	[NH ₄ S ₂ O ₇]	Micelle size at 45 °C (nm)	Micellar cavity at 45 °C (nm)	Crystal size (nm)	Basal spacing (nm)	Layers number
0.0125	0.12	0.47	0.02	9	6–7	3.0	0.73	5 ± 0
0.025	0.12	0.47	0.02	9	6–7	3.1	0.73	5 ± 0
0.025	0.053	0.47	0.02	9	6–7	4.3	0.73	7 ± 0
0.05	0.053	0.35	0.025	17	14–15	5.8	0.73	9 ± 2
0.065	0.044	0.42	0.025	25	22–23	8.1	0.72	12 ± 2

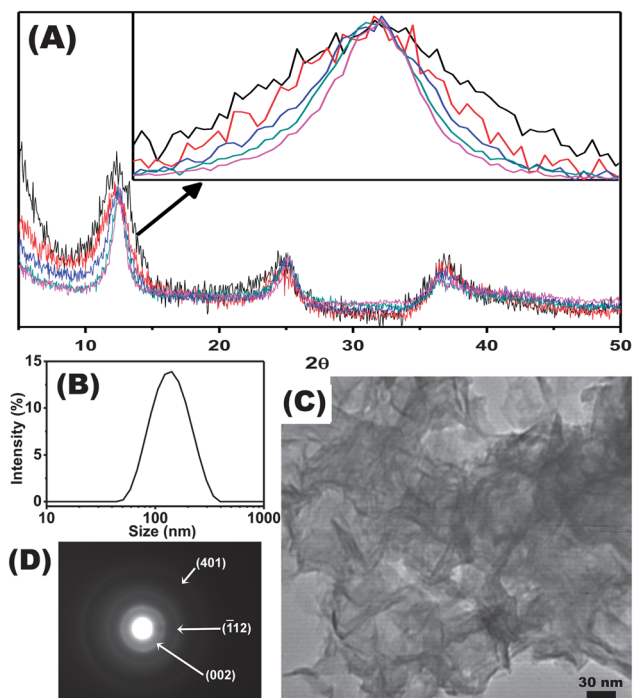


Fig. 2 (A) X-Ray diffraction patterns show only diffraction peaks associated with birnessite. The zoom shows the different broadness (thickness) of the (001) reflection (20 s of accumulation time) associated with sizes from 3.0 (the wider peak) to 8.1 nm (the thinner peak). (B) Hydrodynamic size of birnessites when still dispersed in the organic medium (just before isopropanol addition, see Experimental section for technical details). (C) and (D) Typical TEM pictures and SAED patterns of samples.

thus, assure confidence in the measurements). Furthermore, errors were exploited to our own benefit as they allowed checking the demethylation efficiency for some conditions while limiting the number of experiments. This was possible as differences from different batches caused only differences in thickness (no chemical or basal spacing changes). For example, this was the case for 9 and 11 layer samples (Mn concentration of 0.05 M, see Table 1). We must point out that production of birnessites was not as straightforward as we had anticipated. Specifically, we found lower and upper limits for the formation of birnessites. Slow oxidation (low oxidating/Mn ratios) gives Mn₃O₄ while substantial bubbling marks an upper limit for the amount of H₂O₂ and KOH that can be added. Replacement of H₂O₂ by NH₄S₂O₇ to avoid substantial bubbling is not possible as its

solubility is limited to around 0.025 M (0.8 M in the aqueous component).

3.3. Methylene blue degradation

Discoloration experiments as a function of time were carried out to check for the thickness dependence of MB demethylation. Unless the contrary is stated the experiments were carried out using a KH₂PO₄ buffer (pH = 7). We, thus, assure a constant pH and avoid possible deintercalation associated with K⁺ concentration gradients. Prior to carrying out absorbance experiments that involve solution/solid separation (centrifugation/filtering), a possible power law dependence of absorbance with wavelength was checked in birnessite suspensions for regions where only scattering contributes to the total attenuation coefficient. We found an inverse-square dependence (Fig. 3) that allowed carrying out measurements at short times (subtraction of scattering) without the problems associated with centrifugation (slow processing, and separation of adsorption and discoloration

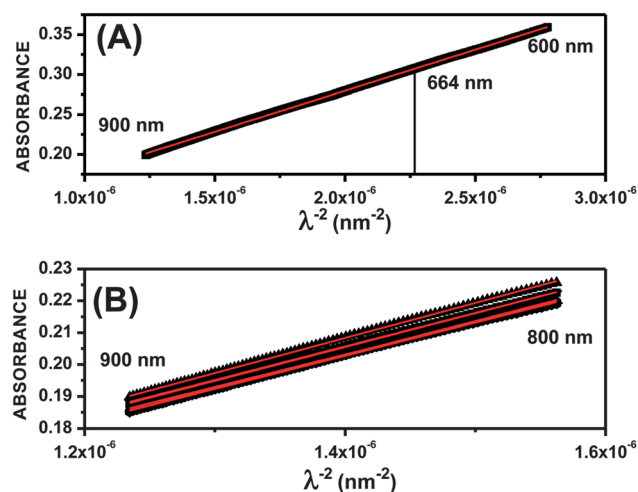


Fig. 3 (A) and (B) show the λ^{-2} scattering dependence of absorbance for aqueous suspensions containing only birnessites and MB/birnessites (variations of 0.03 in scattering are within the experimental error). While Fig. 3A shows that the λ^{-2} dependence extends well beyond 664 nm (maximum for MB absorption), Fig. 3B shows the same linear dependence when MB is added (registered in the region where no absorbance of MB is detected). Scattering at 664 nm was therefore extrapolated from the linear region. The experiments were carried out for a solid concentration of 0.8 mg mL⁻¹ and a MB concentration of 2.5×10^{-4} M. The suspensions were diluted 1 : 35 before registering the UV/Vis spectrum.

effects) or filtration (we observed systematic dye retention in filters). Subtraction was possible as the absorbance maximum for MB (664 nm) is located at a region where the total attenuation coefficient of birnessites is only the result of scattering.

Fig. 4A clearly shows that the discoloration efficiency strongly increases with the decrease in thickness in a margin of 7 octahedral layers. Fig. 4A also shows that drying leads to a total loss of efficiency due to the formation of irreversible aggregates during drying (see for example TEM in Fig. 2C). We also observe in Fig. 4A a loss of efficiency in experiments involving a 5 layer sample in which a cationic polyelectrolyte (PDDA, polydiallyldimethylammonium chloride) was added. This result indicates that large cations cannot be present in solution if degradation of MB is required. As mentioned in the Introduction there exists substantial evidence that surface mechanisms are involved in the oxidative degradation of organic compounds by manganese oxides; therefore large cations compete with MB for all of the adsorption sites and demethylation efficiency decreases. The implication of this result is that methods to control the thickness based on monosheets which are obtained *via* exfoliation using large cations,^{10,22,23} followed by electrostatically driven layer-by-layer growth using cationic polyelectrolytes,²⁴ must not be applied if MB demethylation is required.

3.4. Mechanism of methylene blue degradation and comparison with electrodeposited thin films

The strong dependence of discoloration with thickness, aggregation and the presence of bulky cations clearly points to a mechanism in which MB is only adsorbed onto the external surface (*i.e.* not intercalated in the birnessites). The absence of changes in the position of diffraction peaks further confirmed this mechanism. This strong dependence with parameters related to exposed surfaces such as thickness and aggregation can explain why particulate birnessites have only been considered for dye sequestration purposes and not as an efficient demethylating agent in the absence of oxidants.^{8,9} Demethylation of MB was

confirmed by the blue shift associated with this process (Fig. 4B), and the formation of the fully demethylated form of MB, which is called thionin, for the most efficient birnessites (Fig. 4C). Assuming that adsorption rates are high and charge compensation coming from MB is significant (we are dealing with few-layer birnessites) there might be a possible increase in discoloration efficiency if K^+ gradients were established. Experimentally, this theory can be checked by simply replacing a KH_2PO_4 by a NaH_2PO_4 buffer while keeping the pH (pH = 7) constant. The result is that a significant increase in efficiency was observed (Fig. 4A). This result brings to our attention that care must be taken when registering and comparing discoloration efficiencies in ultrathin birnessites. In any case, when compared to thin films,⁷ the high loading capabilities of concentrated aqueous suspensions containing birnessites make it possible to discolor 10-fold larger amounts of MB (2.5×10^{-4} vs. 3.1×10^{-5} in thin films) at similar times (3 h). It is important to remark that we limited the solid concentration of birnessites to values able to be monitored by visible spectrophotometry with adequate precision. Of course if we had prepared more concentrated suspensions larger amounts of MB would have been demethylated or the time taking to demethylate the same amount would have been shorter.

Finally, and only with the aim of making some comparison with the mechanism proposed for demethylation in the absence of oxidants for electrodeposited thin films, some kinetic parameters were derived from the samples that show sufficient number of data at the shortest times to get a statistically reliable fit and statistically reliable differences between samples (Fig. 4D). A pseudo-first order process was detected for the samples with thicknesses changing from 9 to 12 layers with a pseudo-first order constant value increasing as expected from 12 to 9 layers (0.6×10^{-3} and $3.5 \times 10^{-3} \text{ min}^{-1}$). This pseudo-first order process along with the absence of Mn cations in solution after MB degradation, the above-mentioned strong dependence with parameters related with available surface sites, and the formation of thionin point to the mechanism proposed for electrodeposited

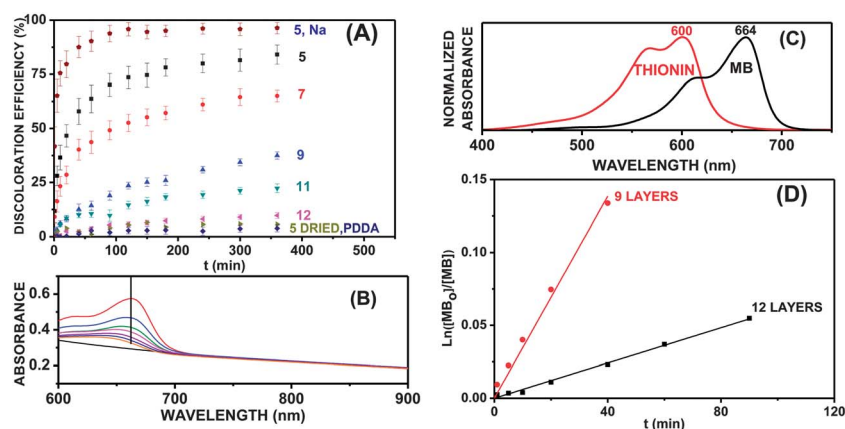


Fig. 4 (A) Discoloration efficiency ($(A_0 - A) \times 100/A_0$) as a function of time and the number of layers (5 to 12 layers) for K-birnessites. Three extra 5 layer samples are included (dried, PDDA 10^{-5} M, and NaH_2PO_4 buffer of pH = 7). The error bar represents the average of 5 different preparations. The error bar was not estimated in the dried sample since milling is far from assuring homogeneity at the level of the non-dried preparations. (B) Typical evolution of absorbance with time (birnessite the “substrate” is also included). (C) Normalized absorbance for methylene blue (MB) and MB after full demethylation (thionin formation) produced by the most efficient of the birnessites (spectrum taken after centrifugation, drying and further dissolution). (D) Pseudo-first order kinetic plot of $\ln[MB]$ as a function of time for samples with 9 and 12 layers. All the experiments were carried out for a solid concentration of 0.8 mg mL^{-1} and a MB concentration of 2.5×10^{-4} M. The suspensions were diluted 1 : 35 before registering the UV/Vis spectrum.

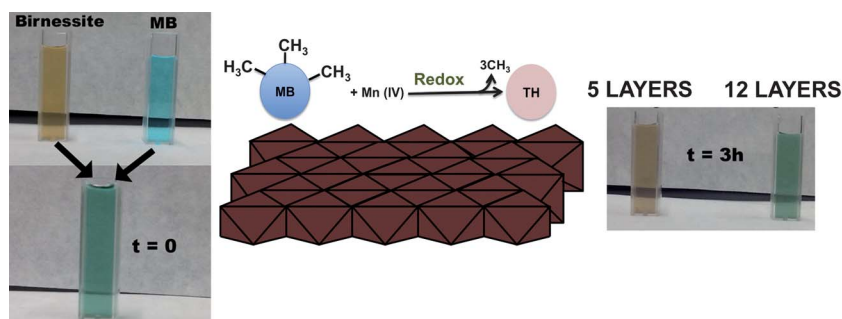


Fig. 5 Schematic representation of the mechanism proposed for complete demethylation of methylene blue (MB) to give thionin (TH) in the presence of colloidal birnessites and in the absence of oxidants. As explained in the main text the mechanism is similar to that reported for electrodeposited thin films. The strong dependence with parameters related to available surface sites (number of octahedral layers per particle) is clearly visualized.

thin films for MB demethylation.⁷ Briefly, adsorption of the MB is followed by demethylation induced by reduction of Mn(IV) to give Mn(III) species. These Mn(III) species can either form a complex with the organic moieties or be reoxidized to Mn(IV) to proceed with the demethylation process (Fig. 5).

Conclusions

We have described a soft-template method for the synthesis of layered manganate (K_xMnO_2 , birnessites) compounds. The method allows a relatively good control at the nanoscale regime on the number of octahedral layers (thickness) in a layered compound of interest in energy and environmental applications. Visual inspection (Fig. 5) and spectroscopic monitoring (Fig. 4A) make clear that the birnessites here obtained can efficiently demethylate MB and that there is a strong dependence of this demethylation with thickness and aggregation (*i.e.* with exposed surfaces). This strong dependence among other things explains why particulate birnessites have only been considered for dye sequestration purposes and not as an efficient discoloration agent in the absence of oxidants. It is quite interesting to remark that experimental errors in this method are minimized (especially in the most efficient birnessites) by the layered structure of the material. Basically, layered structures cannot contain a non-integer number of layers; in other words, layered structures introduce quantization effects.

Acknowledgements

The financial support from the Ministerio of Economía and Competitividad (MAT2008-03224) is gratefully acknowledged.

References

- J. Liu, J. P. Durand, L. Espinal, L. J. Garces, S. Gomez, Y.-C. Son, J. Villegas and S. L. Suib, Layered Manganese Oxides: Synthesis, Properties, and Applications, in *Handbook of Layered Materials*, ed.
- S. M. Auerbach, K. A. Carrado and P. K. Dutta, Marcel Dekker, New York, 2004, ch. 9, pp. 475–508.
- R. Ma and T. Sasaki, *Adv. Mater.*, 2010, **22**, 5082.
- A. Takagaki, C. Tagusagawa, S. Hayashi, M. Hara and K. Domen, *Energy Environ. Sci.*, 2010, **3**, 82.
- X. Lang, A. Hirata, T. Fujita and M. Chen, *Nat. Nanotechnol.*, 2011, **6**, 232.
- W. Yan, T. Ayvazian, J. Kim, Y. Liu, K. C. Donovan, W. Xing, Y. Yang, J. C. Hemminger and R. M. Penner, *ACS Nano*, 2011, **5**, 8275.
- T. Sriskandakumar, N. Opembe, C.-H. Chen, A. Morey, C. Kingodu and S. L. Suib, *J. Phys. Chem. A*, 2009, **113**, 1523.
- M. Zaied, S. Peulon, N. Bellakahl, B. Desmazieres and A. Chause, *Appl. Catal., B*, 2011, **101**, 441.
- M. A. Al-Ghouthi, Y. S. Al-Degs, M. A. M. Khraisheh, M. N. Ahmad and S. J. Allen, *J. Environ. Manage.*, 2009, **90**, 3520.
- L. Zhang, Y. Nie, C. Hu and X. Hu, *J. Hazard. Mater.*, 2011, **190**, 780.
- K. Kai, Y. Yoshida, H. Kageyama, G. Saito, T. Ishigaki, Y. Furukawa and J. Kawamata, *J. Am. Chem. Soc.*, 2008, **130**, 15938.
- S. Stroes-Gascoyne, Adsorption behaviour of delta-manganese dioxide in relation to its use as a resin in trace metal speciation studies, Open access dissertations and theses, paper 3899, 1983.
- D.-Y. Sung, I. Y. Kim, T. W. Kim, M.-S. Song and S.-J. Hwang, *J. Phys. Chem. C*, 2011, **115**, 13171.
- O. Prieto, M. Del Arco and V. Rives, *J. Mater. Sci.*, 2003, **38**, 2815.
- M.-S. Song, K. M. Lee, Y. R. Lee, I. Y. Kim, T. W. Kim, J. L. Gunjekar and S.-J. Hwang, *J. Phys. Chem. C*, 2010, **114**, 22134.
- S. Ching, J. A. Landrigan and M. L. Jorgensen, *Chem. Mater.*, 1995, **7**, 1604.
- A. T. Stone and J. J. Morgan, *Environ. Sci. Technol.*, 1984, **18**, 617.
- D. G. Shchukin and G. B. Sukhorukov, *Adv. Mater.*, 2004, **16**, 671.
- J. C. Ravey, M. Buzier and C. Picot, *J. Colloid Interface Sci.*, 1984, **97**, 9.
- C.-L. Chang and H. S. Fogler, *Langmuir*, 1997, **13**, 3295.
- P. Tartaj and C. J. Serna, *J. Am. Chem. Soc.*, 2003, **125**, 15754.
- J. L. Lemyre, S. Lamarre, A. Beaupre and A. M. Ritcey, *Langmuir*, 2010, **26**, 10524.
- Y. Omomo, T. Sasaki, L. Z. Wang and M. Watanabe, *J. Am. Chem. Soc.*, 2003, **125**, 3568.
- Y. Oaki and H. Imai, *Angew. Chem., Int. Ed.*, 2007, **46**, 4951.
- L. Z. Wang, Y. Omomo, N. Sakai, K. Fukuda, I. Nakai, Y. Ebina, K. Takada, M. Watanabe and T. Sasaki, *Chem. Mater.*, 2003, **15**, 2873.